JPEDAV (2004) 25:437-447
DOI: 10.1361/15477030420926
1547-7037/$19.00 ©ASM International

Study of the La_2O_3-Ga_2O_3 System by Experiment and Thermodynamic Calculations

M. Zinkevich, S. Geupel, H. Nitsche, M. Ahrens, and F. Aldinger

(Submitted November 13, 2003; in revised form July 21, 2004)

Thermodynamic and phase diagram experimental data relevant to the La_2O_3-Ga_2O_3 system have been critically assessed. The system is characterized by the presence of two stoichiometric, congruently melting compounds $LaGaO_3$ and $La_4Ga_2O_9$, each occurring in two polymorphic modifications. A number of key experiments have been carried out to measure the heat capacity and to characterize phase transitions in both compounds as well as to determine the solubility of La in Ga_2O_3 and that of Ga in La_2O_3. These data were used together with information from the literature to generate self-consistent thermodynamic description of the La_2O_3-Ga_2O_3 system.

1. Introduction

Solid oxide fuel cells (SOFCs) continue to attract interest as a potentially reliable, durable, and inexpensive technology for generating electricity from hydrocarbon fuels [2001Ste, 2001Ral]. The state-of-the-art SOFC systems use yttria-stabilized zirconia (YSZ) as electrolyte, which requires the working temperature around 1273 K to achieve sufficient power density. Using other types of solid electrolytes with higher oxide-ion conductivity is a possibility to increase the SOFC performance at reduced operating temperatures (773-1073 K). Perovskite-like solid solutions with a general formula $La_{1-x}Sr_xGa_{1-y}Mg_yO_{3-z}$ (LSGM) are considered as possible new electrolyte materials [1994Ish, 2001Hua]. These compounds are pure ionic conductors over a wide range of oxygen partial pressures and show sufficiently high conductivity at 973 K, which is comparable to that of YSZ at 1273 K. At present, the preparation of single-phase LSGM materials is difficult because the phase relations in the quaternary La_2O_3-SrO-Ga_2O_3-MgO system are unknown. For the time- and cost-effective optimization of LSGM composition, it is essential to evaluate the thermodynamic stability of various phases. Then, by minimizing the Gibbs energy of a system under the given set of conditions using a numerically sophisticated procedure, phase equilibria of interest can be calculated. This technique is known as the CALPHAD method and has been successfully used in the past for the design of multicomponent alloys and ceramics [1970Kau, 1998Sau, 1998Yok]. This work is a part of a project to derive a self-consistent set of Gibbs energy functions describing the La_2O_3-SrO-Ga_2O_3-MgO system and is focused on the binary subsystem La_2O_3-Ga_2O_3.

M. Zinkevich, S. Geupel, H. Nitsche, and **F. Aldinger,** Max-Planck-Institut für Metallforschung, Heisenbergstraße 3, D-70569 Stuttgart, Germany; and **M. Ahrens,** Max-Planck-Institut für Festkörperforschung, Heisenbergstraße 1, D-70569 Stuttgart, Germany. Contact e-mail: zinkevich@mf.mpg.de.

2. Assessment of the Literature Information

2.1 Solid Phases

The binary La_2O_3-Ga_2O_3 system was studied by several techniques and for different ranges of composition and temperature. Two stable, congruently melting compounds have been observed (Table 1): $LaGaO_3$ and $La_4Ga_2O_9$ (or $2La_2O_3 \cdot Ga_2O_3$). At room temperature and ambient pressure, $LaGaO_3$ has a distorted perovskite structure with tilting of the GaO_6 octahedra, resulting in an orthorhombic unit cell (space group *Pbnm*). The presence of an anomaly on the thermal expansion curve near 420 K, indicative of a possible phase transition in $LaGaO_3$, has been discovered by Sandstrom and coworkers [1988San]. Miyazawa [1989Miy] observed a surface roughening of a polished $LaGaO_3$ substrate caused by a ferroelastic-like phase transition at 413-423 K. Subsequent studies using x-ray and neutron diffraction as well as the transmission electron microscopy at high temperatures [1991Wan, 1991Kob, 1992Mor, 1993Bdi, 1994Mar], dilatometry [1990Bry, 2000Hay, 2001Ale, 2001Ina], differential scanning calorimetry [1990Bry, 1991Kob, 1994Dub], and differential thermal analysis [2001Ler] confirmed the presence of a structural phase transition into the rhombohedral polymorph around 420 K, which is accompanied by an endothermic effect and a volume shrinkage. The phase transition in $LaGaO_3$ can also be induced by the application of pressure, as revealed by [2001Ken] who found that the *Pbnm* $\rightarrow$ $R\bar{3}c$ transition does occur reversibly around 2 GPa at room temperature. Geller observed a phase transition in $LaGaO_3$ at about 1150 K in his early studies based on x-ray powder diffraction photographs and differential thermal analysis [1957Gel, 1970Gel]. Recent reports are, however, in agreement on the lower transition temperature. The temperature dependence of the rhombohedral angle was monitored to indicate that the material retains the rhombohedral structure up to its melting point [1990Bry]. At the same time, Kobayashi and coworkers detected a broad enthalpy change starting around 1020 K by differential scanning calorimetry (DSC) measurement [1991Kob] and assigned it to a second-order phase

Table 1 Solid phases in the La_2O_3-Ga_2O_3 system

Phase (stability range at P = 1 bar)	Pearson symbol	Space group	Prototype	Lattice parameters(a)	Reference
β-Ga_2O_3	*mC*20	*C*2/*m*	β-Ga_2O_3	a = 1.2214(3) nm b = 0.30371(9) nm c = 0.57981(9) nm β = 103.83(2)°	[1996Ahm]
A-La_2O_3 (T < 2313 K)	*hP*5	$P\bar{3}m1$	La_2O_3	a = 0.39381(3) nm c = 0.61361(6) nm γ = 120°	[1979Ald] [1966Foe]
H-La_2O_3 (T = 2313 to 2383 K)	*hP*10	$P6_3/mmc$	La_2O_3	a = 0.4057(2) nm c = 0.6430(3) nm γ = 120°	[1979Ald] [1966Foe]
X-La_2O_3 (T > 2383 K)	*cI*8	$Im\bar{3}m$	$LaYbO_3$	a = 0.451(1) nm	[1979Ald] [1966Foe]
LGO-$LaGaO_3$ (T < 420 K)	*oP*20	*Pbnm*	$GdFeO_3$	a = 0.55227(1) nm b = 0.54908(1) nm c = 0.77725(1) nm	[2001Ler]
LGR-$LaGaO_3$ (T > 420 K)	*hR*30	$R\bar{3}c$	$LaAlO_3$	a = 0.55899(1) nm c = 1.36279(3) nm	[2001Ler]
LGM1-$La_4Ga_2O_9$ (T < 1544 K)	*mP*60	$P2_1/c$	$Eu_4Al_2O_9$	a = 0.79724(4) nm b = 1.11964(5) nm c = 1.16184(6) nm β = 109.462(4)°	[1995Yam]
LGM2-$La_4Ga_2O_9$ (T > 1544 K)	*mP*60	$P2_1/c$	$Y_4Al_2O_9$	…	[1995Yam]

(a) Lattice parameters refer to 298 K (β-Ga_2O_3, A-La_2O_3, LGO-$LaGaO_3$, LGM1-$La_4Ga_2O_9$), 2323 K (H-La_2O_3), 2473 K (X-La_2O_3), and 1073 K (LGR-$LaGaO_3$)

transition, with the structure being monoclinically distorted above the transition temperature, as revealed by x-ray powder diffraction. In contrast, Aleksandrovskii et al., [2001Ale] claimed that this phase transition is of first order.

The crystal structure of $La_4Ga_2O_9$ has been analyzed by Yamane and coworkers [1995Yam]. It is found to be isotypic to that of $Eu_4Al_2O_9$ [1969Bra]. The lattice parameters of the monoclinic unit cell (space group $P2_1/c$) obtained from Rietveld refinement of x-ray powder diffraction data are given in Table 1. High-temperature differential scanning calorimetry and dilatometry revealed that $La_4Ga_2O_9$ exhibits a reversible phase transition at 1544 K with a volume shrinkage on heating and thermal hysteresis [1995Yam]. The crystal structure of the high-temperature phase has not been studied yet. However, isostructural $Y_4Al_2O_9$ phase (YAM) is known to undergo a diffusionless, martensitic phase transition at 1643 K into a monoclinic high-temperature phase having the same space group [1998Yam].

Antic-Fidancev et al. [1997Ant] have noticed the existence of a ternary $LaGa_3O_6$ phase crystallizing in the monoclinic space group *P*2/*m*. Unfortunately, the authors provide neither lattice parameters nor atomic coordinates of the hypothetical $LaGa_3O_6$ phase. Since the details of sample preparation and structure determination are also missing, the existence of the $LaGa_3O_6$ phase has to be considered as doubtful.

In the following, low-temperature orthorhombic $LaGaO_3$, high-temperature rhombohedral $LaGaO_3$, low-temperature monoclinic $La_4Ga_2O_9$, and high-temperature monoclinic $La_4Ga_2O_9$ are abbreviated as LGO, LGR, LGM1, and LGM2, respectively (Table 1).

2.2 Phase Diagram

A schematic La_2O_3-Ga_2O_3 phase diagram below 1773 K has been first reported by Schneider et al. [1961Sch]. It shows $LaGaO_3$ and $La_4Ga_2O_9$ compounds and the phase transition in $LaGaO_3$ adopted from Geller [1957Gel]. Mizuno and coworkers [1985Miz] reported a tentative phase diagram of La_2O_3-Ga_2O_3 system above 1473 K in air, and this diagram has been accepted in subsequent works [1999Hro, 2001Maj1, 2001Maj2]. The liquidus temperatures have been measured across the whole range of compositions, but the polymorphism of the $LaGaO_3$ and $La_4Ga_2O_9$ is not taken into account. Their melting points are reported to be 1988 ± 20 K and 1977 ± 20 K, respectively. The phase diagram shows three eutectic points at 1618, 1923, and 1943 K with 23, 57, and 80 mol% of La_2O_3, respectively (Table 2). Kuncewicz-Kupczyk et al. [2002Kun] reproduced the La_2O_3-Ga_2O_3 phase diagram of Mizuno and coworkers [1985Miz] with an addition of a phase boundary just below 1200 K (in the composition range from 0 to 66.7 mol% La_2O_3). This line is also shown in [1961Sch] and obviously corresponds to the temperature of phase transition in $LaGaO_3$ reported in [1957Gel]. The solid solubility of La in Ga_2O_3 of about 6-7 mol% has been

Table 2 Invariant reactions in the La_2O_3-Ga_2O_3 system

Reaction	La_2O_3, mol%			*T*, K	Reference
Eutectic:	23	0	50	1618 ± 20	[1985Miz]
Liquid ↔ β-Ga_2O_3 + LGR	22.3	0	50	1596	This work
Congruent:	50	50	…	1988 ± 20	[1985Miz]
LGR ↔ Liquid	50	50	…	1953	This work
Eutectic:	57	50	66.7	1943 ± 20	[1985Miz]
Liquid ↔ LGR + LGM2	56.7	50	66.7	1932	This work
Congruent:	66.7	66.7	…	1977 ± 20	[1985Miz]
LGM2 ↔ Liquid	66.7	66.7	…	1977	This work
Eutectic:	80	100	66.7	1923 ± 20	[1985Miz]
Liquid ↔ A-La_2O_3 + LGM2	72.3	100	66.7	1962	This work
Polymorphic:	50	50	…	420 ± 5	[1990Bry]
LGO ↔ LGR					[1991Wan]
					[1991Kob]
					[1992Mor]
					[1993Bdi]
					[1994Mar]
					[1994Dub]
					[2000Hay]
					[2001Ale]
					[2001Ina]
					[2001Ler]
	50	50	…	414 ± 3	This work
Polymorphic:	66.7	66.7	…	1544	[1995Yam]
LGM1 ↔ LGM2	66.7	66.7	…	1558 ± 5	This work

determined by Majewski and coworkers [2001Maj1, 2001Maj2].

2.3 Thermodynamic Data

The standard Gibbs energy of formation of $LaGaO_3$ from its constituent sesquioxides according to the reaction: 0.5 A-La_2O_3 + 0.5 β-Ga_2O_3 → LGR has been determined twice [1991Aza, 2000Jac]. The values given by [1991Aza] and [2000Jac] at 950 K deviate significantly from each other, although both measurements were carried out using the electromotive force (emf) technique based on a CaF_2 solid electrolyte. However, as shown by Jacob et al. [2000Jac] the LaF_3/La_2O_3 reference electrode used in [1991Aza] is unstable against formation of a single-phase oxyfluoride solid solution, leading to an incorrect value of the Gibbs energy of formation of $LaGaO_3$.

In a recent vaporization study of the La_2O_3-Ga_2O_3 system, the thermodynamic activities of La_2O_3 and Ga_2O_3 have been determined between 1600 and 1900 K [2002Kun]. The activity of Ga_2O_3 results directly from the ion intensities by measuring successively the samples and pure Ga_2O_3 as reference. The activity of La_2O_3 in the two-phase fields of the La_2O_3-Ga_2O_3 system was then evaluated with the use of Gibbs-Duhem integration. The Gibbs energy of formation of $LaGaO_3$ at 1700 K calculated in [2002Kun] is significantly more negative than that given by [2000Jac] at 950 K.

By means of high-temperature solution calorimetry using a $2PbO \cdot B_2O_3$ solvent at 977 K, the enthalpy of formation of $LaGaO_3$ from its sesquioxides was determined as $\Delta_f H = -50.86 \pm 2.92$ kJ/mol [1998Kan]. The entropy of formation of $LaGaO_3$ was deduced to be negative. Taking the $\Delta_f G$ value of [2002Kun], the entropy of formation is calculated as $\Delta_f S = -2.6 \pm 2.5$ J/mol · K, if one ignores the temperature dependence of $\Delta_f H$ and $\Delta_f S$. This would be consistent with the observation that an entropy change near zero is characteristic for the formation of perovskites from their oxide components [1975Sch]. The low-temperature specific heat of $LaGaO_3$ has been measured by [2000Bar] and showed no anomalies below 298 K.

Only a few data are available for the $La_4Ga_2O_9$ phase. From the thermodynamic activities [2002Kun], the Gibbs energy of formation of $La_4Ga_2O_9$ at 1700 K was calculated as $\Delta_f G = -99.2 \pm 7.9$ kJ/mol.

3. Description of Key Experiments

A careful analysis of the literature information for the La_2O_3-Ga_2O_3 system revealed that a dataset, which is needed to understand the system comprehensively and to perform a thermodynamic assessment is still incomplete. Therefore, a number of key experiments have been performed. Firstly, the solubility of La in Ga_2O_3 and that of Ga in La_2O_3 has been accurately determined. Secondly, phase transitions in $LaGaO_3$ and $La_4Ga_2O_9$ have been characterized and the corresponding enthalpy changes have been measured. Thirdly, the heat capacity of both compounds has been measured over a wide range of temperatures.

Samples with nominal La:Ga atomic ratio of 15:85, 1:3, 1:1, 2:1, and 85:15 were prepared using powders of La_2O_3 and Ga_2O_3 (Sigma Aldrich GmbH, Steinheim, Germany; purity > 99.99%). The powders were mixed and ground in ethanol using an agate ball mill, dried at 338 K and calcined at 1273 K in air for 12 h. The calcined powders were ground in an agate mortar, cold isostatically pressed into pellets at 625 MPa (1 min), and sintered at 1573-1873 K, in air for 24 h, with intermediate regrinding and pressing. Finally, the samples were furnace cooled to room temperature. Phase identifications were performed using scanning electron microscopy (SEM) in the backscattered electron imaging mode with energy-dispersive x-ray analysis (EDX; Model DSM 982 Gemini, Karl Zeiss, Inc., Oberkochen, Germany) at 20 kV and 10 nA, with a standard error of ±0.5 wt.% and a Co Kα line calibration element, and x-ray diffractometry (XRD; Model D5000, Siemens AG, Karlsruhe, Germany) with position-sensitive detector (PSD), Cu Kα radiation, $2\Theta = 10°$ to 100°, $\Delta 2\Theta = 0.008°$, and a counting time of 3 s. Phase transitions in $LaGaO_3$ and $La_4Ga_2O_9$ were characterized by dilatometry (differential push-rod dilatometer; Model DIL802, Bähr-Thermoanalyse GmbH, Hüllhorst, Germany) with sapphire as a reference and DSC (Models Pyris 1, Perkin-Elmer Instruments, Norwalk, CT, between 323 and 873 K and MHTC96, SETARAM S.A., Caluire, France, between 473 and 1673 K) calibrated with In, Li_2SO_4, Ag, and Au standards. The linear thermal expansion coefficient was calculated as $\alpha = (1/l_0)(dl/dT)$ where l_0

Table 3 Results of the phase analysis in sintered La_2O_3-Ga_2O_3 samples

La:Ga ratio	Sintering temperature, K	Phases observed by XRD and EDX	Solid solubilities from EDX (La in Ga_2O_3, Ga in La_2O_3), mol%
15:85	1573	β-Ga_2O_3 + LGO	0.6 ± 0.3
	1623	β-Ga_2O_3 + LGO	0.3 ± 0.2
	1673	β-Ga_2O_3 + LGO	0.1 ± 0.1
1:3	1623	β-Ga_2O_3 + LGO	…
1:1	1723	LGO	…
2:1	1723	LGM1 + LGR (traces)	…
85:15	1723	A-La_2O_3 + LGM1	0.3 ± 0.5
	1823	A-La_2O_3 + LGM1	0.1 ± 0.2
	1873	A-La_2O_3 + LGM1	0.2 ± 0.3

and l are the lengths of a sample at room temperature and at the temperature T (K), respectively. The low-temperature specific heat of $LaGaO_3$ and $La_4Ga_2O_9$ between 1.5 and 305 K was measured by means of a home-made high-precision calorimeter applying Nernst's quasi-adiabatic step heating method [1987Gme, 1992Ota]. The sample holder was a 0.1 mm thick sapphire disk supporting the heater (evaporated stainless steel, ~2 kΩ) and a commercially calibrated resistance thermometer (depending on the range of temperature either CERNOX or Pt100). The 300-600 mg samples were cemented to the sample holder using a weighed amount of Apiezon-N (Apiezon Products Ltd., London, UK) grease. The contributions of grease and sapphire disc to the specific heat were subtracted to obtain the net sample values. Heat capacity above room temperature was measured by power-compensated (T < 873 K) and heat-flow DSC (up to 1673 K) using a sapphire sample or a high-purity α-Al_2O_3 powder, respectively, as standard reference materials for the caloric calibration.

4. Results of Experimental Study and Their Discussion

Results of the phase analysis in sintered La_2O_3-Ga_2O_3 samples are given in Table 3. The sample with La:Ga ratio of 1:1 shows the presence of the LGO phase only. Almost pure LGM1 phase is obtained at La:Ga = 2:1, but a few additional peaks are detected, which correspond to the LGR phase. The content of this impurity phase is estimated to be lower than 5 wt.% and in the further experimental studies this sample is considered as single LGM1 phase. Samples with La:Ga = 15:85 and 1:3 show a characteristic β-Ga_2O_3 + LGO two-phase microstructure (Fig. 1a and b), while A-La_2O_3 and LGM1 phases are found at La:Ga = 85:15 composition (Fig. 1c). Both the $LaGaO_3$ and $La_4Ga_2O_9$ are confirmed to be stoichiometric; i.e., the La:Ga atomic ratio is measured as 1.00 ± 0.05 and 2.00 ± 0.05, respectively, in all samples. The solid solubility of La in Ga_2O_3 and that of Ga in La_2O_3 is obviously below the limit of detection at all sintering temperatures (Table 3), so that it can be considered as negligible. The relatively large solid solubility of La in

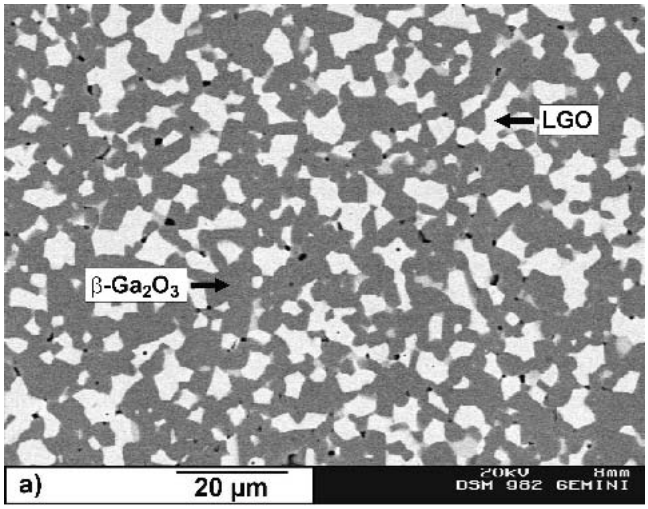

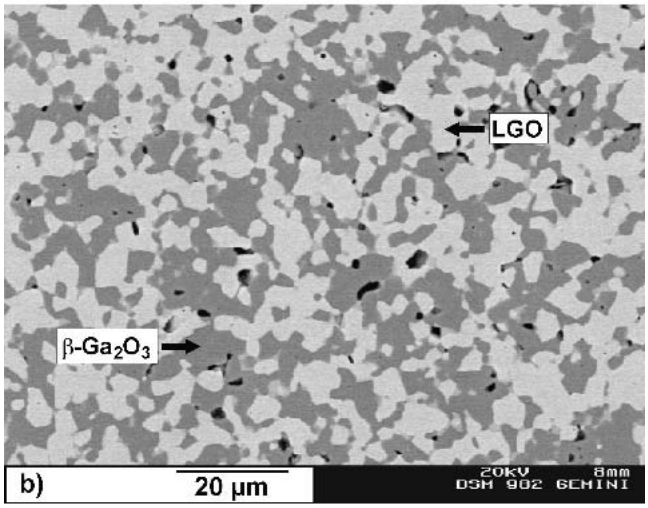

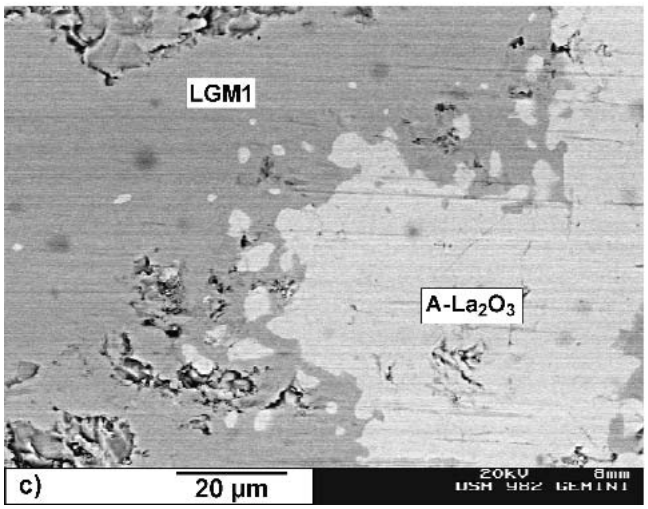

Fig. 1 SEM micrographs of the La_2O_3-Ga_2O_3 samples with La:Ga atomic ratio of **(a)** 15:85, **(b)** 1:3, and **(c)** 85:15 sintered at 1623 K (a) and (b) and 1723 K (c)

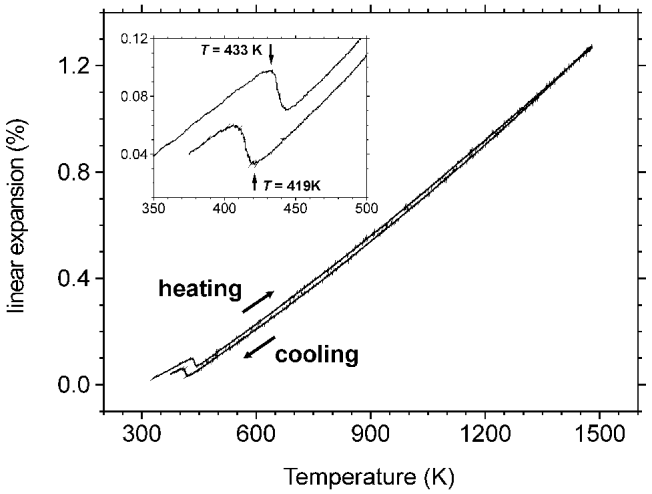

Fig. 2 Thermal expansion of $LaGaO_3$ in air; heating and cooling with 5 K/min, sample length: 6.236 mm. The inset shows a region around the phase transition.

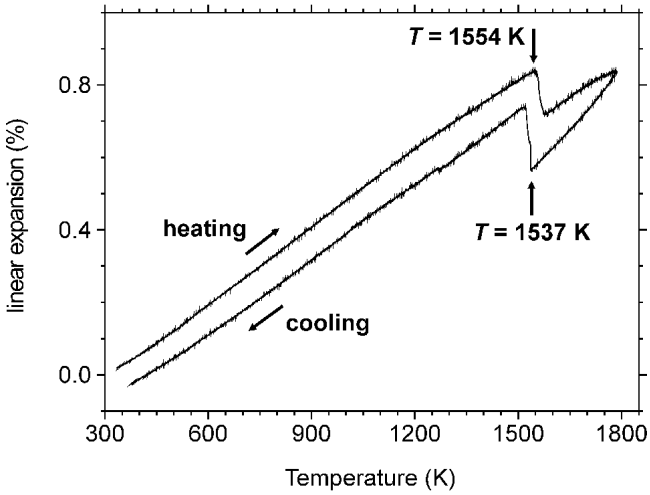

Fig. 3 Thermal expansion of $La_4Ga_2O_9$ in air. Heating and cooling with 5 K/min, sample length: 5.515 mm

Ga_2O_3 of 6-7 mol% reported in [2001Maj1, 2001Maj2] is thus not confirmed. It can also hardly be expected considering the differences in crystal structures of β-Ga_2O_3 and A-La_2O_3 and in the ionic radii of La^{3+} and Ga^{3+}.

Figures 2 and 3 show the dilatometric curves of the $LaGaO_3$ and $La_4Ga_2O_9$, respectively. On heating, the LGO phase undergoes a first-order phase transition at 433 K into the LGR modification, which is accompanied by a linear shrinking of about 0.03% (Fig. 2). The reverse LGR → LGO transformation on cooling occurs at 419 K and results in an abrupt increase in length. Further either first- or second-order phase transitions at least up to 1473 K can be ruled out due to the absence of any other steps or kinks on the thermal expansion curve (Fig. 2). The linear thermal expansion coefficient of the LGR phase between 450 and 1473 K is well described by:

$$\alpha(T) = 7.367 \times 10^{-6} + 6.407 \times 10^{-9}\, T - 1.915 \times 10^{-12}\, T^2\ (\mathrm{K}^{-1})$$

The numerical values calculated from this equation are in good agreement with those reported in the literature at the corresponding temperatures [1988San, 2000Hay]. The available literature data for the volume change are compiled in Table 4. The dilatometric measurements on single crystals are not considered here, since the thermal expansion of $LaGaO_3$ is known to be strongly anisotropic [1990Bry]. All values are in fair agreement, except the data of [1991Wan].

The LGM1 phase shows a first-order phase transition on heating at 1554 K into the LGM2 modification, which is accompanied by a linear shrinking of about 0.14% (Fig. 3). On cooling, a sudden expansion takes place at 1537 K, which indicates the LGM2 → LGM1 transformation. No other phase transitions in $La_4Ga_2O_9$ can be seen from the thermal expansion curves. Similar observations have been made by Yamane and coworkers [1995Yam] in their dilatometric study. The average linear thermal expansion coefficient of the LGM1 phase between 500 and 1500 K is (6.0 ± 0.5) × 10^{-6}/K. The thermal expansion behavior of the LGM2 phase is similar (Fig. 3), but the accurate determination of the α-value is not possible in this case.

Table 4 Volume change at the orthorhombic-to-rhombohedral phase transition in $LaGaO_3$

Experimental technique	Volume change, ΔV_{tr}, cm^3/mol	Reference
XRD	–0.30	[1991Wan]
	–0.07	[1991Kob]
Dilatometry(a)	–0.043	[2000Hay]
	–0.018	[2001Ale]
XRD	–0.050	[2001Ken]
Dilatometry(a)	–0.032	This work

(a) Calculated using the value of 0.23654 nm^3 as the unit cell volume of the orthorhombic LGO phase at 413 K [1994Mar]

Figure 4 shows DSC traces on heating the $LaGaO_3$ sample between 390 and 450 K. An endothermic effect at 414 K due to the LGO → LGR phase transition is clearly observed. The variation of the onset temperature with increasing heating rate from 5-40 K/min is within 1 K (Fig. 4). Thermal cycling produced very similar (almost overlapping) curves that demonstrate a complete reversibility of a phase transition (Fig. 4). The enthalpy change is calculated as 305 ± 5 J/mol. This is to compare with 355 J/mol reported by O'Bryan and coworkers [1990Bry]. The difference can be considered as acceptable, taking into account the different sample preparation (single crystal versus powder).

Examples of DSC curves, which are obtained around the phase transition in $La_4Ga_2O_9$ are shown in Fig. 5. The endothermic peak confirms the occurrence of the LGM1 → LGM2 first-order phase transition. Compared with $LaGaO_3$, a higher sample weight was used to provide enough sensitivity, and, hence, a significant dependence of the transition

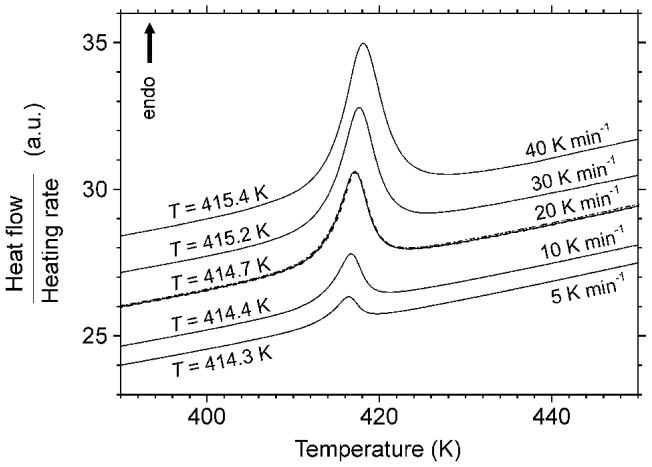

Fig. 4 DSC data for $LaGaO_3$ sample (40.611 mg) on heating with different rates in argon. The onset temperatures of phase transition are indicated. At 20 K/min a superposition of four consecutive measurements is shown.

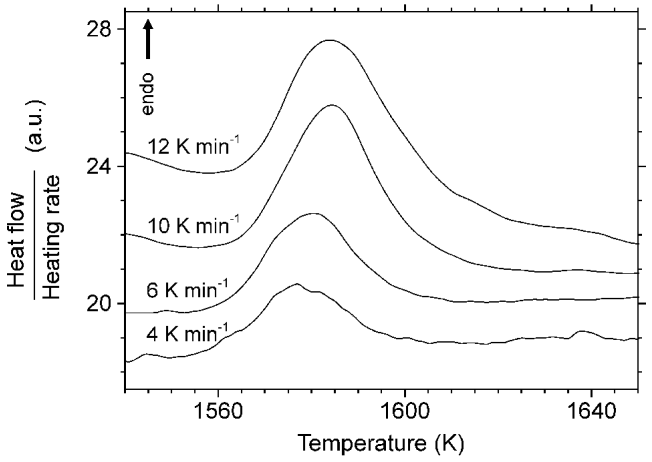

Fig. 5 DSC data for $La_4Ga_2O_9$ sample (946.6 mg) on heating with different rates in air

temperature on the heating rate was observed. Extrapolation to the heating rate of zero gives the onset temperature of 1558 K, which is believed to be close to the transition point, if the sample would be in thermal equilibrium. An enthalpy change shows no clear dependence on the heating rate and a value of 2100 ± 200 J/mol is calculated from 10 independent measurements.

The observed negative change of the molar volume upon the transitions from low- to high-temperature phase in $LaGaO_3$ and $La_4Ga_2O_9$ along with the positive enthalpy change is typical for Y- and rare-earth aluminates and gallates [1988San, 1991Kob, 1995Yam, 2000Hay, 2001Ale, 2001Ina]. It is also consistent with the reported decrease of the transition temperature in $LaGaO_3$ with increasing pressure [2001Ken] in accordance with the Clausius-Clapeyron equation. However, such behavior is not in line with a general trend: the high-temperature phase tends to have greater openness of structure and lower coordination, so that a positive volume change is expected [1978Rao]. The origin of the volume reduction in $LaGaO_3$ can be understood, if the tolerance factor

$$t = \frac{1}{\sqrt{2}} \frac{d_{AO}}{d_{BO}}$$

is considered as a relevant parameter for estimating the degree of distortion in a perovskite ABO_3, where d_{AO} and d_{BO} are the average bond distances [1970Goo]. The stability of a structure increases as t approaches unity. The LGO → LGR phase transition is then energetically favored since it is accompanied by an increase of the tolerance factor from 0.9483 to 0.9904, respectively [1994Mar]. At the same time, the average bond distances in LaO_{12} and GaO_6 polyhedra show discontinuous decrease at the phase transition. Similar observations have been made by Oikawa and coworkers [2000Oik] for the isostructural perovskite-like compound $LaCrO_3$. Neutron diffraction revealed that the volume compression of $LaCrO_3$ caused by the orthorhombic-to-rhombohedral phase transition at 523 K is principally due to the shrinking of the CrO_6 octahedron. Such rearrangement of structure results in increase of tolerance factor, which is necessary to stabilize the rhombohedral phase.

Generalizing the above conclusion, one can postulate that the volume compression upon phase transition from low- to high-temperature modification can be expected in geometrically constrained structures. Compounds $R_4M_2O_9$ (R = Y, La-Yb, M = Al, Ga) undoubtedly fall into this category.

Figure 6(a) shows the heat capacity data for $LaGaO_3$. Compared with the literature data [2000Bar], somewhat higher values are measured in the current study. This small difference (about 5 J/mol · K = 20 J/mg · K at 300 K) may be due to the different apparatus, level of impurities, and/or preparation conditions. Apart from a very sharp peak due to the LGO → LGR phase transition no anomalies on the heat capacity curve are observed (Fig. 6a). Heat capacity of $La_4Ga_2O_9$ is measured for the first time in this work and is plotted in Fig. 6(b). A quite regular behavior is seen, except for the peak at high temperature, which is caused by the LGM1 → LGM2 phase transition. The enthalpy changes due to the LGO → LGR and LGM1 → LGM2 phase transitions determined by the integration of the heat capacity data are 340 and 2200 J/mol, respectively. These values are in good agreement with DSC measurements (Table 5).

The heat capacities of both the LGO and LGR phases and the LGM1 phase were fitted by:

$$C_P(T) = -c - 2dT - 6eT^2 - 2fT^{-2} \quad \text{(Eq 1)}$$

The enthalpy, entropy, and Gibbs energy are then represented as follows [1991Din]:

$$H(T) = a - cT - dT^2 - 2eT^3 + 2fT^{-1} \quad \text{(Eq 2)}$$

$$S(T) = -b - c - c \ln(T) - 2dT - 3eT^2 + fT^{-2} \quad \text{(Eq 3)}$$

$$G(T) = a + bT + cT \ln(T) + dT^2 + eT^3 + fT^{-1} \quad \text{(Eq 4)}$$

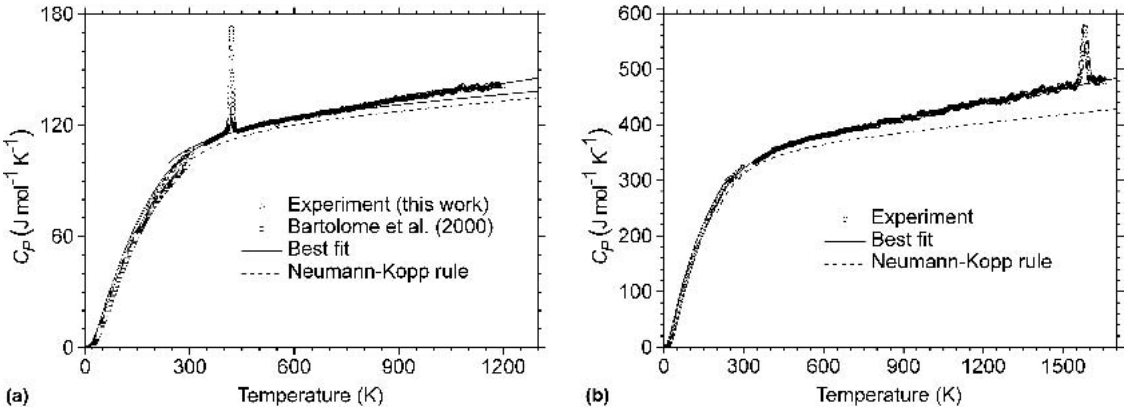

Fig. 6 Heat capacity data for **(a)** $LaGaO_3$ and **(b)** $La_4Ga_2O_9$. Fitting function is given by Eq 1; the coefficients *c* to *f* can be extracted from Table 6 using Eq 4 and 1.

Table 5 Experimental thermodynamic data for the La_2O_3-Ga_2O_3 system

Data description	Experimental technique(b)	Measured value	Reference	Calculated value(a)
0.5 A-La_2O_3 + 0.5 β-Ga_2O_3	emf (T = 1040 K)	−46.2 ± 4.5	[2000Jac]	−51.864
→ LGR, $\Delta_t H$ (kJ/mol)	SC (T = 977 K)	−50.86 ± 2.92	[1998Kan]	−52.329
LGO → LGR,	DSC (T = 418 K)	+355	[1990Bry]	+305
$\Delta_{tr}H$ (J/mol)	DSC (T = 414 K)	+305 ± 5	This work	+305
LGO, S (J/mol · K)	AC (T = 306 K)	109.6 ± 2	This work	111.9
LGM1 → LGM2, $\Delta_{tr}H$ (J/mol)	DSC (T = 1558 K)	+2100 ± 200	This work	+2101
LGM1, S (J/mol · K)	AC (T = 305 K)	363.4 ± 5	This work	362.4
β-Ga_2O_3 + LGR, a(La_2O_3)	…	$(1.4 \pm 0.7) \times 10^{-3}$	[2002Kun]	5.1×10^{-5}
LGR + LGM2, a(La_2O_3)	KEMS	0.64 ± 0.32	[2002Kun]	0.130
LGR + LGM2, a(Ga_2O_3)	(T = 1700 K)	$(2.2 \pm 0.8) \times 10^{-3}$	[2002Kun]	3.9×10^{-4}
LGM2 + A-La_2O_3, a(Ga_2O_3)	…	$(8.9 \pm 3.3) \times 10^{-4}$	[2002Kun]	6.6×10^{-6}

(a) According to the present assessment.
(b) AC, adiabatic calorimetry; DSC, differential scanning calorimetry; emf, electromotive force measurement; KEMS, Knudsen effusion mass spectrometry; SC, solution calorimetry

Care has been taken to ensure the monotonic growth of the heat capacity functions (solid lines in Fig. 6) up to 6000 K, which is generally taken as a high-temperature limit in thermodynamic databases [1991Din]. Parameters for the LGO phase have been adjusted under constraint that beyond its stability range (i.e., for $T > 414$ K), C_P values are lower than those for the stable LGR phase at same temperatures. This guarantees that LGO phase does not appear again in the calculated diagram (see below) at high temperatures. The heat capacity of the LGM2 phase is measured in a very narrow interval of temperatures (Fig. 6b), so that it is represented by the same function as for LGM1 phase. Heat capacities calculated for the mechanical mixtures of A-La_2O_3 and β-Ga_2O_3 in the corresponding proportions are also shown in Fig. 6 for comparison. It can be seen that the empirical Neumann-Kopp rule (an assumption for zero heat capacity of formation) is not fulfilled in both cases, while the measured heat capacity is always higher.

Expressions for the entropy of the LGO and LGM1 phases were obtained combining the coefficients form corresponding heat capacity functions (Eq 1) with the entropy values at 306 K (LGO, S = 109.6 J/mol · K) and 305 K (LGM1, S = 363.4 J/mol · K), which are calculated by the numerical integration under the curve C_P/T versus T according to the third law of thermodynamics. The expressions for the high-temperature modifications, LGR and LGM2 were then evaluated using the entropy increments at the phase transitions LGO → LGR (ΔS = 0.74 J/mol · K) and LGM1 → LGM2 (ΔS = 1.35 J/mol · K), which are calculated from their enthalpies (ΔH) and temperatures (T_{tr}), taking into account that $\Delta G(T_{tr}) = \Delta H - T_{tr}\Delta S = 0$.

5. Thermodynamic Models

The essential feature of the CALPHAD method is the analytical representation of the Gibbs energy of individual phases in a system in terms of state variables, such as temperature, pressure, and composition (thermodynamic description). Some of these expressions contain adjustable coefficients (model parameters). The optimal values of the unknown parameters providing the best match between the calculated quantities and their experimental counterparts are usually obtained by the weighted nonlinear least squares minimization procedure (thermodynamic optimization), using experimental thermochemical, constitutional (phase dia-

gram), and crystallographic data as input. The selection of the model for a phase must be based on the physical and chemical properties of that phase, most importantly crystallography, type of bonding, ordering, defect structure, etc.

Since the solid solubility of La in Ga_2O_3 and that of Ga in La_2O_3 is found to be negligible (Table 3), the Gibbs energy of A-La_2O_3, H-La_2O_3, X-La_2O_3, and β-Ga_2O_3 is adopted from the recent assessments of binary systems La-O and Ga-O, respectively [2001Gru, 2004Zin]. The Gibbs energy of the stoichiometric compounds LGO, LGR, LGM1, and LGM2 is given by Eq 4.

The liquid phase is described by the two-sublattice model for ionic liquids [1985Hil], assuming that the anions and cations occupy separate sublattices and are allowed to mix freely therein. In the La_2O_3-Ga_2O_3 system, the liquid is represented as $(Ga^{3+}, La^{3+})_2(O^{2-})_3$ and the molar Gibbs energy is given by:

$$G^{liq} = y_{La^{3+}} {}^{\circ}G^{liq}_{La_2O_3} + y_{Ga^{3+}} {}^{\circ}G^{liq}_{Ga_2O_3} + 2RT(y_{La^{3+}} \ln y_{La^{3+}} + y_{Ga^{3+}} \ln y_{Ga^{3+}}) + {}^{E}G^{liq} \quad \text{(Eq 5)}$$

where y_i represents the site fraction of the species i on the cation sublattice, ${}^{\circ}G^{liq}_{La_2O_3}$ and ${}^{\circ}G^{liq}_{Ga_2O_3}$ equal the Gibbs energy of liquid binary oxides, respectively [2001Gru, 2004Zin], and ${}^{E}G^{liq}$ is the excess Gibbs energy, which can be expressed as a power series in terms of y_i using the compound energy formalism [2001Hil]:

$${}^{E}G^{liq} = y_{Ga^{3+}} y_{La^{3+}} \sum_{\nu=0}^{n} {}^{\nu}L^{liq}_{Ga^{3+},La^{3+}:O^{2-}} (y_{Ga^{3+}} - y_{La^{3+}})^{\nu} \quad \text{(Eq 6)}$$

The colons separate species on different sublattices. The terms ${}^{\nu}L^{liq}_{Ga^{3+}:La^{3+}:O^{2-}}$ are so-called interaction parameters of an order ν, which account for the deviation from the ideal mixing behavior between La^{3+} and Ga^{3+}. It can be shown that ionic liquid model in the La_2O_3-Ga_2O_3 system is identical to a simple substitutional model $(La_2O_3,Ga_2O_3)_1$, when site fractions of cations are replaced by mole fractions of oxides, i.e., $y_{La^{3+}} = x_{La_2O_3}$ and $y_{Ga^{3+}} = x_{Ga_2O_3}$.

6. Optimization and Calculations

The thermodynamic model parameters of the La_2O_3-Ga_2O_3 system were evaluated using the optimization module PARROT of the multicomponent software for the thermodynamic calculations "Thermo-Calc" [2002The] on the base of all available experimental data: liquidus [1985Miz], invariant reactions (Table 2), heat capacity measured in this work, and other thermodynamic properties (Table 5). The temperatures of polymorphic transformations of $LaGaO_3$ and $La_4Ga_2O_9$ are adopted from the present calorimetric study (see above). For the LGO, LGR, LGM1, and LGM2 compounds, only two coefficients of Eq 4, a and b were adjusted, while the coefficients c, d, and f were determined from the best fit of the heat capacity curve. The coefficient e was fixed to zero. The Gibbs energy of the liquid phase is described with the use of two interaction parameters ${}^{0}L^{liq}_{Ga^{3+},La^{3+}:O^{2-}}$ and ${}^{1}L^{liq}_{Ga^{3+},La^{3+}:O^{2-}}$; both depend linearly on the temperature. The optimized thermodynamic parameters are listed in Table 6.

Figure 7 shows the calculated La_2O_3-Ga_2O_3 phase dia-

Table 6 Summary of the thermodynamic parameters describing the La_2O_3-Ga_2O_3 system referred to stable element reference H^{SER} (T = 298.15 K, P = 1 bar)

Parameter	Equation	Reference
Liquid $(Ga^{3+},La^{3+})_2(O^{2-})_3$		
${}^{\circ}G^{liq}_{La_2O_3} = -1{,}812{,}300 + 1285.34\,T - 200\,T\ln T$	5	[2001Gru]
${}^{\circ}G^{liq}_{Ga_2O_3} = -1{,}027{,}472 + 636.2433\,T - 112.3935\,T\ln T - 0.00796268819\,T^2 + 1{,}080{,}114\,T^{1}$	5	[2004Zin]
${}^{0}L^{liq}_{Ga^{3+},La^{3+}:O^{2-}} = -72{,}987.0 + 107.1263\,T$	6	This work
${}^{1}L^{liq}_{Ga^{3+},La^{3+}:O^{2-}} = -198{,}305.6 + 100.2462\,T$	6	This work
A-La_2O_3 $(La^{3+})_2(O^{2-})_3$		
${}^{\circ}G^{A}_{La_2O_3} = -1{,}835{,}600 + 674.72\,T - 118\,T\ln T - 0.008\,T^2 + 620{,}000\,T^{-1}$	4	[2001Gru]
H-La_2O_3 $(La^{3+})_2(O^{2-})_3$		
${}^{\circ}G^{H}_{La_2O_3} = -1{,}789{,}600 + 654.83\,T - 118\,T\ln T - 0.008\,T^2 + 620{,}000\,T^{-1}$	4	[2001Gru]
X-La_2O_3 $(La^{3+})_2(O^{2-})_3$		
${}^{\circ}G^{X}_{La_2O_3} = -1{,}729{,}600 + 629.65\,T - 118\,T\ln T - 0.008\,T^2 + 620{,}000\,T^{-1}$	4	[2001Gru]
β-Ga_2O_3 $(Ga^{3+})_2(O^{2-})_3$		
${}^{\circ}G^{\beta}_{Ga_2O_3} = -1{,}127{,}917 + 684.8332\,T - 112.3935\,T\ln T - 0.00796268819\,T^2 + 1{,}080{,}114\,T^{-1}$	4	[2004Zin]
LGO $(La^{3+})_1(Ga^{3+})_1(O^{2-})_3$		
${}^{\circ}G_{LGO} = -1{,}538{,}543.1 + 701.7736\,T - 118.996196\,T\ln T - 0.00784817227\,T^2 + 837{,}025.375\,T^{-1}$	4	This work
LGR $(La^{3+})_1(Ga^{3+})_1(O^{2-})_3$		
${}^{\circ}G_{LGR} = -1{,}533{,}711.7 + 638.9024\,T - 109.728653\,T\ln T - 0.0139853325\,T^2 + 476{,}583.792\,T^{-1}$	4	This work
LGM1 $(La^{3+})_4(Ga^{3+})_2(O^{2-})_9$		
${}^{\circ}G_{LGM1} = -4{,}909{,}105.3 + 1971.5304\,T - 340.312645\,T\ln T - 0.0425340414\,T^2 + 1{,}987{,}936.32\,T^{-1}$	4	This work
LGM2 $(La^{3+})_4(Ga^{3+})_2(O^{2-})_9$		
${}^{\circ}G_{LGM2} = -4.907{,}004.0 + 1970.1818\,T - 340.312645\,T\ln T - 0.0425340414\,T^2 + 1{,}987{,}936.32\,T^{-1}$	4	This work

Note: Values are given in SI units (Joule, mole, and Kelvin). Equation indicates the equation number in the text.

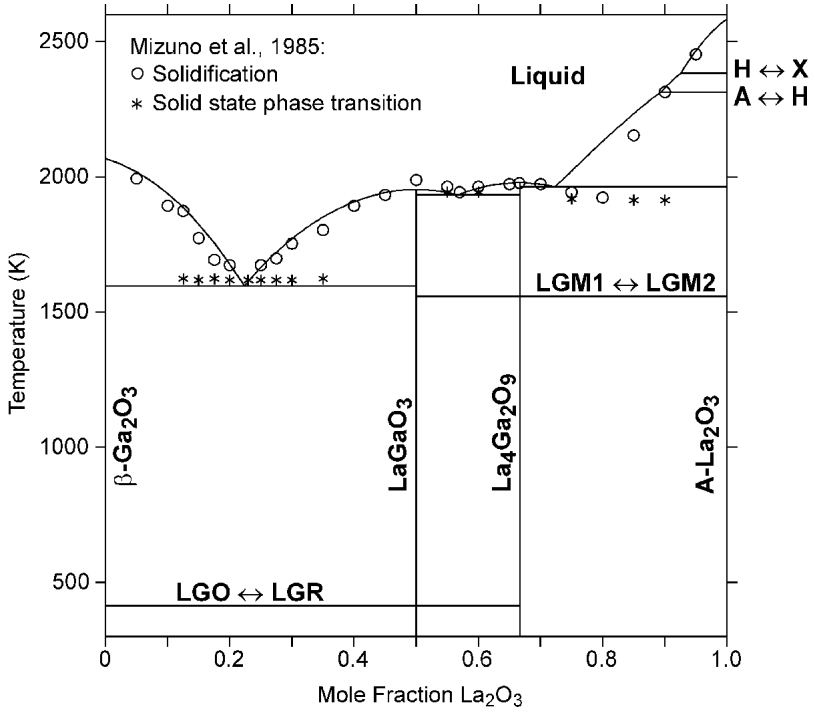

Fig. 7 Calculated La_2O_3-Ga_2O_3 phase diagram with experimental measurements superimposed

gram along with the experimental liquidus measurements of Mizuno and coworkers [1985Miz]. There is a significant improvement over the phase diagrams available in the literature. None of the reported diagrams [1961Sch, 1985Miz, 2002Kun] cover the full range from room temperature to the liquidus. The phase diagram shown by Schneider et al. [1961Sch] is only schematic. The phase diagram of Mizuno et al. [1985Miz] does not take the polymorphism of La_2O_3, $LaGaO_3$, and $La_4Ga_2O_9$ into account, while both phase diagrams shown in [1961Sch] and [2002Kun] incorporate incorrect temperature for the phase transition in $LaGaO_3$ (1150 K). The revised phase diagram (Fig. 7) shows two horizontal lines in the subsolidus region at 414 and 1558 K (Table 2), which are the correct temperatures for the phase transitions in $LaGaO_3$, and $La_4Ga_2O_9$, respectively.

The solidification and invariant points given in [1985Miz] are well reproduced and a good quantitative agreement exists, except for the composition range between 75 and 85 mol% of La_2O_3. The deviations in the measured and calculated temperatures of the La_2O_3-liquidus may have different origins. Firstly, one may speculate about lower accuracy in determination of solidification temperatures above 2000 K. Secondly, a dissolution of Ga in high-temperature polymorphs of La_2O_3, which is not taken into account in the present thermodynamic description could result in their extended stability far below the temperatures of the corresponding phase transitions in pure La_2O_3. A wide region of the La_2O_3-based solid solutions is, however hardly to be formed due to the large misfit in the ionic radii of La^{3+} and Ga^{3+}. Thirdly, the calculated liquidus curve for La_2O_3-rich compositions ($\geq$75 mol%, Fig. 7) is essentially determined by the difference in the Gibbs energy of A-La_2O_3 and the liquid lanthanum sesquioxide. Experimental thermodynamic data are, however available only for A-La_2O_3. The assessed Gibbs energy functions of H-, X-, or liquid La_2O_3 [2001Gru] are therefore based on the estimated values for enthalpy of the phase transitions A $\rightarrow$ H, H $\rightarrow$ X, and X $\rightarrow$ liquid, respectively. Given the unknown reliability of such estimations, one may attempt to determine the corresponding enthalpies from the liquidus curves in the known binary systems of La_2O_3 with other oxides. For example, to fit all the liquidus data in the La_2O_3-Ga_2O_3 system, the difference in the enthalpy of liquid La_2O_3 and the A-form should be noticeably reduced from +181 kJ/mol [2001Gru] to about +73 kJ/mol. However, the uncertainty of the enthalpy determined by this method depends strongly on experimental errors in the determination of liquidus.

In Table 2, the calculated temperatures and compositions at the invariant reactions in the La_2O_3-Ga_2O_3 system are compared with experimental data. Most of the calculated values are within the limits of experimental errors. Larger deviation exists for the temperature and composition of the eutectic Liquid $\leftrightarrow$ A-La_2O_3 + LGM2, due to the problem with La_2O_3-liquidus, as described above. The congruent melting point of LGR phase is calculated at 1953 K that makes a difference of 35 K. Although it is not very large compared with the experimental error (±20 K) it is worth noting that a better fit of this temperature is impossible without disturbing the neighboring liquidus curves and invariant reactions.

Table 5 shows calculated and experimental thermodynamic properties of phases and phase mixtures in the La_2O_3-Ga_2O_3 system. It can be seen that enthalpies of formation and entropies of $LaGaO_3$ and $La_4Ga_2O_9$ as well as the en-

thalpies of phase transitions are very well reproduced. At the same time, the calculated activities of Ga_2O_3 and La_2O_3 in the two-phase fields are significantly lower than those derived from vaporization study [2002Kun].

From the known enthalpy and volume change the expected shift of the LGO → LGR phase transition temperature with increasing pressure can be calculated by integration of the Clausius-Clapeyron equation:

$$\frac{dP}{dT} = \frac{\Delta H_{tr}}{T \Delta V_{tr}} \quad \text{(Eq 7)}$$

Neglecting the temperature and pressure dependencies of ΔH_{tr} and ΔV_{tr} one obtains

$$P_2 - P_1 = \ln\left(\frac{T_2}{T_1}\right) \frac{\Delta H_{tr}}{\Delta V_{tr}} \quad \text{(Eq 8)}$$

where T_1 and T_2 are the transition temperatures at pressures P_1 and P_2, respectively. The mean volume change of $-(4.3 \pm 2) \times 10^{-8}$ m^3/mol can be calculated from Table 4 excluding the data of [1991Wan]. With ΔH_{tr} = +305 J/mol, T_1 = 414 K, P_1 = 0.1 MPa, and T_2 = 298 K, Eq 8 then gives P_2 = 2.3 GPa. This value is in excellent agreement with experimental observation that pressure-induced orthorhombic-to-rhombohedral phase transition in $LaGaO_3$ occurs between 1.83 and 2.5 GPa at room temperature [2001Ken].

7. Conclusions

The La_2O_3-Ga_2O_3 system is assessed by experiment and thermodynamic calculation. The solid solubility of La in Ga_2O_3 and that of Ga in La_2O_3 is negligible. Temperatures and enthalpies of the reversible first-order phase transitions in $LaGaO_3$ (orthorhombic to rhombohedral) and $La_4Ga_2O_9$ (monoclinic to unknown structure) are reliably determined. The volume change at these phase transitions is negative. Heat capacity of both compound is measured in a wide temperature range. Thermodynamic properties of the La_2O_3-Ga_2O_3 system are analyzed by means of the CALPHAD method and a self-consistent thermodynamic description is obtained. The calculated phase diagram and thermodynamic properties are in reasonable agreement with experiments.

Acknowledgment

The authors are grateful to Mr. E. Schmitt for technical assistance.

References

1957Gel: S. Geller, Crystallographic Studies of Perovskite-Like Compounds. 4. Rare Earth Scandates, Vanadites, Galliates, Orthochromites, *Acta Crystallogr.,* Vol 10 (No. 4), 1957, p 243-248

1961Sch: S.J. Schneider, R.S. Roth, and J.L. Waring, Solid State Reactions Involving Oxides of Trivalent Cations, *J. Research Natl. Bur. Standards,* Vol 65A (No. 4), 1961, p 345-374

1966Foe: M. Foex and J.P. Traverse, Investigations About Crystalline Transformation in Rare Earths Sesquioxides at High Temperatures, *Rev. Int. Hautes Temp. Refract.,* Vol 3 (No. 4), 1966, p 429-453 (in French)

1969Bra: C.D. Brandle and H. Steinfink, Crystal Structure of $Eu_4Al_2O_9$, *Inorg. Chem.,* Vol 8 (No. 6), 1969, p 1320-1324

1970Gel: S. Geller and P.M. Raccah, Phase Transitions in Perovskite-Like Compounds of Rare Earths, *Phys. Rev. B,* Vol 2 (No. 4), 1970, p 1167-1171

1970Goo: J.B. Goodenough and J.M. Longo, Crystallographic and Magnetic Properties of Perovskite and Perovskite-Related Compounds, *Magnetic and Other Properties of Oxides and Related Compounds,* K.H. Hellwege and A.M. Hellwege, Ed., Springer, Berlin, Germany, 1970, Chapter 3, p 126

1970Kau: L. Kaufman and H. Bernstein, *Computer Calculation of Phase Diagrams,* Academic Press, 1970

1975Sch: H. Schmalzried and A. Navrotsky, in *Festkörperthermodynamik. Chemie des festen Zustandes,* Verlag Chemie, Weinheim, 1975, p 128 (in German)

1978Rao: C.N.R. Rao and K.J. Rao, in *Phase Transitions in Solids,* McGraw-Hill, London, 1978, p 42

1979Ald: P. Aldebert and J.P. Traverse, Study by Neutron-Diffraction of High-Temperature Structures of La_2O_3 and Nd_2O_3, *Mater. Res. Bull.,* Vol 14 (No. 3), 1979, p 303-323 (in French)

1985Hil: M. Hillert, B. Jansson, B. Sundman, and J. Ågren, A Two-Sublattice Model for Molten Solutions With Different Tendency for Ionization, *Metall. Trans.,* Vol 16A, 1985, p 261-266

1985Miz: M. Mizuno, T. Yamada, and T. Ohtake, Phase Diagram of the System Ga_2O_3-La_2O_3 at High Temperatures, *J. Ceram. Soc. Jpn.,* Vol 93 (No. 6), 1985, p 295-300 (in Japanese)

1987Gme: E. Gmelin, Low-Temperature Calorimetry—A Particular Branch of Thermal-Analysis, *Thermochim. Acta,* 1987, Vol 110, p 183-208

1988San: R.L. Sandstrom, E.A. Giess, W.J. Gallagher, A. Segmuller, E.I. Cooper, M.F. Chisholm, A. Gupta, S. Shinde, and R.B. Laibowitz, Lanthanum Gallate Substrates for Epitaxial High-Temperature Superconducting Thin-Films, *Appl. Phys. Lett.,* Vol 53 (No. 19), 1988, p 1874-1876

1989Miy: S. Miyazawa, Surface Roughening Associated With ~140 °C Transition of a $LaGaO_3$ Substrate for High-T_C Superconducting Films, *Appl. Phys. Lett.,* Vol 55 (No. 21), 1989, p 2230-2232

1990Bry: H.M. O'Bryan, P.K. Gallagher, G.W. Berkstresser, and C.D. Brandle, Thermal-Analysis of Rare-Earth Gallates and Aluminates, *J. Mater. Res.,* 1990, Vol 5 (No. 1), p 183-189

1991Aza: A.M. Azad, R. Sudha, and O.M. Sreedharan, Thermodynamic Stability of $LaGaO_3$ and Its Compatibility With $YBa_2Cu_3O_{7-x}$ for Substrate Application, *Mater. Res. Bull.,* Vol 26 (No. 1), 1991, p 97-105

1991Din: A.T. Dinsdale, SGTE Data for Pure Elements, *CALPHAD,* Vol 15 (No. 4), 1991, p 317-425

1991Kob: J. Kobayashi, Y. Tazoh, M. Sasaura, and S. Miyazawa, Structural-Analysis of Lanthanum Gallate, *J. Mater. Res.,* Vol 6 (No. 1), 1991, p 97-100

1991Wan: Y. Wang, X. Liu, G.D. Yao, R.C. Liebermann, and M. Dudley, High-Temperature Transmission Electron-Microscopy and X-Ray-Diffraction Studies of Twinning and the Phase-Transition at 145 °C in $LaGaO_3$, *Mater. Sci. Eng. A—Struct. Mater. Prop. Microstruct. Process.,* Vol 132, 1991, p 13-21

1992Mor: A.N. Morozov, O.Y. Morozova, N.M. Ponomarev, and S.N. Knyazev, Structural Perfection of $LaGaO_3$ Single Crystals—A New Substrate Material for Growing High-T_C Super-

conducting Films, *Sverkhprovodimost', Fizika, Khimiya, Tekhnika,* Vol 5 (No. 2), 1992, p 388-399 (in Russian)

1992Ota: S.B. Ota and E. Gmelin, Improved Analysis of Isoperibol Heat-Pulse Calorimetry, *Meas. Sci. Technol.,* Vol 3 (No. 11), 1992, p 1047-1049

1993Bdi: I.K. Bdikin, I.M. Shmytko, A.M. Balbashov, and A.V. Kazansky, Twinning of $LaGaO_3$ Single-Crystals, *J. Appl. Crystallogr.,* Vol 26, 1993, p 71-76

1994Dub: D.C. Dube, H.J. Scheel, I. Reaney, M. Daglish, and N. Setter, Dielectric-Properties of Lanthanum Gallate ($LaGaO_3$) Crystal, *J. Appl. Phys.,* Vol 75 (No. 8), 1994, p 4126-4130

1994Ish: T. Ishihara, H. Matsuda, and Y. Takita, Doped $LaGaO_3$ Perovskite Type Oxide as a New Oxide Ionic Conductor, *J. Am. Chem. Soc.,* Vol 116 (No. 9), 1994, p 3801-3803

1994Mar: W. Marti, P. Fischer, F. Altorfer, H.J. Scheel, and M. Tadin, Crystal-Structures and Phase-Transitions of Orthorhombic and Rhombohedral $RGaO_3$ (R = La, Pr, Nd) Investigated by Neutron Powder Diffraction, *J. Phys.-Condes. Matter,* Vol 6 (No. 1), 1994, p 127-135

1995Yam: H. Yamane, K. Ogawara, M. Omori, and T. Hirai, Phase-Transition of Rare-Earth Aluminates $Re_4Al_2O_9$ and Rare-Earth Gallates $Re_4Ga_2O_9$, *J. Am. Ceram. Soc.,* Vol 78 (No. 9), 1995, p 2385-2390

1996Ahm: J. Ahman, G. Svensson, and J. Albertsson, A Reinvestigation of β-Gallium Oxide, *Acta Crystallogr. Sect. C-Cryst. Struct. Commun.,* Vol 52, 1996, p 1336-1338

1997Ant: E. Antic-Fidancev, M. Lemaitre-Blaise, M. Latroche, P. Porcher, J. Coutures, and J.P. Coutures, Optical Study of a New Phase $LaGa_3O_6$, Re^{3+} (Re = Pr, Nd, Eu) in the La_2O_3-Ga_2O_3 System, *J. Alloys Compd.,* Vol 250 (No. 1-2), 1997, p 342-346

1998Kan: Y. Kanke and A. Navrotsky, A Calorimetric Study of the Lanthanide Aluminum Oxides and the Lanthanide Gallium Oxides, Stability of the Perovskites and the Garnets, *J. Solid State Chem.,* Vol 141 (No. 2), 1998, p 424-436

1998Sau: N. Saunders and A.P. Miodownik, *CALPHAD Calculation of Phase Diagrams,* Pergamon Materials Series, Vol 1, 1998, p 332-344

1998Yam: H. Yamane, M. Shimada, and B.A. Hunter, High-Temperature Neutron Diffraction Study of $Y_4Al_2O_9$, *J. Solid State Chem.,* Vol 141 (No. 2), 1998, p 466-474

1998Yok: H. Yokokawa, Phase Diagrams and Thermodynamic Properties of Zirconia Based Ceramics, *Key Engineering Materials (Switzerland),* Vol 153-154, 1998, p 37-73

1999Hro: M. Hrovat, S. Bernik, J. Holc, and Z. Samardzija, Subsolidus Phase Equilibria in the La_2O_3-Ga_2O_3-NiO System, *J. Mater. Res.,* Vol 14 (No. 6), 1999, p 2351-2354

2000Bar: F. Bartolome, J. Bartolome, M. Castro, and J.J. Melero, Specific Heat and Magnetic Interactions in $NdCrO_3$, *Phys. Rev. B,* Vol 62 (No. 2), 2000, p 1058-1066

2000Hay: H. Hayashi, M. Suzuki, and H. Inaba, Thermal Expansion of Sr- and Mg-Doped $LaGaO_3$, *Solid State Ion.,* Vol 128 (No. 1-4), 2000, p 131-139

2000Jac: K.T. Jacob, N. Dasgupta, H. Näfe, and F. Aldinger, Measurement of Gibbs Energy of Formation of $LaGaO_3$ Using a Composition-Graded Solid Electrolyte, *J. Mater. Res.,* Vol 15 (No. 12), 2000, p 2836-2843

2000Oik: K. Oikawa, T. Kamiyama, T. Hashimoto, Y. Shimojyo, and Y. Morii, Structural Phase Transition of Orthorhombic $LaCrO_3$ Studied by Neutron Powder Diffraction, *J. Solid State Chem.,* Vol 154 (No. 2), 2000, p 524-529

2001Ale: V.V. Aleksandrovskii, N.U. Venskovskii, G.M. Kaleva, E.D. Politova, S.G. Prutchenko, L.A. Rudnitskii, S.Y. Stefanovich, and A.Y. Khortova, Phase Composition, Microstructure, and Thermal Expansion of B_2O_3-Modified $LaGaO_3$-Based Ceramics, *Inorg. Mater.,* Vol 37 (No. 6), 2001, p 641-646

2001Gru: A.N. Grundy, B. Hallstedt, and L.J. Gauckler, Thermodynamic Assessment of the Lanthanum-Oxygen System, *J. Phase Equilib.,* Vol 22 (No. 2), 2001, p 105-113

2001Hil: M. Hillert, The Compound Energy Formalism, *J. Alloys Compd.,* Vol 320 (No. 2), 2001, p 161-176

2001Hua: K.Q. Huang, J.H. Wan, and J.B. Goodenough, Increasing Power Density of LSGM-Based Solid Oxide Fuel Cells Using New Anode Materials, *J. Electrochem. Soc.,* Vol 148 (No. 7), 2001, p A788-A794

2001Ina: H. Inaba, H. Hayashi, and M. Suzuki, Structural Phase Transition of Perovskite Oxides $LaMO_3$ and $La_{0.9}Sr_{0.1}MO_3$ With Different Size of B-Site Ions, *Solid State Ion.,* Vol 144 (No. 1-2), 2001, p 99-108

2001Ken: B.J. Kennedy, T. Vogt, C.D. Martin, J.B. Parise, and J.A. Hriljac, Pressure-Induced Orthorhombic to Rhombohedral Phase Transition in $LaGaO_3$, *J. Phys. Condens. Matter.,* Vol 13 (No. 48), 2001, p L925-L930

2001Ler: M. Lerch, H. Boysen, and T. Hansen, High-Temperature Neutron Scattering Investigation of Pure and Doped Lanthanum Gallate, *J. Phys. Chem. Solids,* Vol 62 (No. 3), 2001, p 445-455

2001Maj1: P. Majewski, M. Rozumek, H. Schluckwerder, and F. Aldinger, Phase Diagram Studies in the Systems La_2O_3-SrO-Ga_2O_3 and La_2O_3-MgO-Ga_2O_3 at 1400 °C in Air, *Int. J. Inorg. Mater.,* Vol 3 (No. 8), 2001, p 1343-1344

2001Maj2: P. Majewski, M. Rozumek, H. Schluckwerder, and F. Aldinger, Phase Diagram Studies in the Systems La_2O_3-SrO-Ga_2O_3 and La_2O_3-MgO-Ga_2O_3 and SrO-MgO-Ga_2O_3 at 1400 °C in Air , *J. Am. Ceram. Soc.*, Vol 84 (No. 5), 2001, p 1093-1096

2001Ral: J.M. Ralph, A.C. Schoeler, and M. Krumpelt, Materials for Lower Temperature Solid Oxide Fuel Cells, *J. Mater. Sci.*, Vol 36 (No. 5), 2001, p 1161-1172

2001Ste: B.C.H. Steel, Material Science and Engineering, The Enabling Technology for the Commercialization of Fuel Cell Systems, *J. Mater. Sci.*, Vol 36 (No. 5), 2001, p 1053-1068

2002Kun: W. Kuncewicz-Kupczyk, D. Kobertz, M. Miller, C. Chatillon, L. Singheiser, and K. Hilpert, Vaporization Studies of the La_2O_3-Ga_2O_3 System, *J. Am. Ceram. Soc.*, Vol 85 (No. 9), 2002, p 2299-2305

2002The: Thermo-Calc User's Guide, Thermo-Calc Software AB (http://www.thermocalc.se), Foundation of Computational Thermodynamics, Stockholm, Sweden, 2002

2004Zin: M. Zinkevich and F. Aldinger, Thermodynamic Assessment of the Gallium-Oxygen System, *J. Am. Ceram. Soc.,* Vol 87 (No. 4), 2004, p 683-691